R.J. Marks II, J.F. Walkup and T.F. Krile, "An improved coherent processor for ambiguity function display", Proceedings of the International Optical Computing Conference, Capri, Italy, September 1976.

AN IMPROVED COHERENT PROCESSOR FOR AMBIGUITY FUNCTION DISPLAY

Robert J. Marks II and John F. Walkup
Department of Electrical Engineering
Texas Tech University
Lubbock, Texas 79409
Thomas F. Krile
Department of Electrical Engineering
Rose-Hulman Institute of Technology
Terre Haute, Indiana 47803

A coherent optical processor for displaying a signal's ambiguity function is described. The required time delay is simulated by 45 degree rotations of two identical input transparencies, and the doppler shift by a subsequent one-dimensional Fourier transformation. The entire ambiguity function is displayed in the output (doppler shift-time delay) plane. Examples of the optically computed ambiguity function for single and double pulse signals are shown to be in excellent agreement with theory. Advantages of this approach over other schemes, and possible extension to real time processing, are also discussed.

Introduction

The ambiguity function, first introduced by Woodward[1], has been applied in radar in predicting the capability of a given signal to simultaneously determine the range and velocity of a target. The range is determined by the time delay, τ, and the velocity by the doppler shift, ν. The ambiguity function for a given signal, $f(t)$, is

$$\chi(\nu,\tau) = \int_{-\infty}^{\infty} f(t)f(t-\tau)\exp(-j2\pi\nu t)\,dt \qquad (1)$$

In optics, Papoulis has employed the ambiguity function in analyzing diffraction phenomena[2].

In this paper, we describe a rather easily implemented coherent processor capable of generating the ambiguity function in magnitude. A similar, yet somewhat more elaborate, scheme for generating $\chi(\nu,\tau)$ in both magnitude and phase is also presented. Such a scheme, for example, would need to be utilized when further coherent processing of the ambiguity function is required.

Cutrona et.al.[3-4] and Preston[5] have proposed a coherent ambiguity function processor[6] which utilizes multiple channels to display the ambiguity function for discrete values of τ. The scheme of Casasent et. al.[7] generates one-dimensional "slices" of the ambiguity function in the (ν,τ) plane. Similar one-dimensional displays have also been electronically produced[8]. Our method, as described in the following sections, (1) displays $|\chi(\nu,\tau)|^2$ in a continuous (rather than quantized) form over the entire (ν,τ) plane, (2) has the capacity for extension to real time processing, and (3) is easily implemented.

Implementation Scheme

The coherent processor capable of displaying the ambiguity function (in magnitude) is pictured in Fig 1. The field amplitude, $U(\nu,\tau)$, in plane P_2 is related to the coherently illuminated transparency, $S(t,\tau)$ in plane P_1 by a one-dimensional Fourier transform:

$$u(\nu,\tau) = \exp(-j2\pi\lambda f\nu^2)\int_{-\infty}^{\infty} S(t,-\tau)\exp(-j2\pi\nu t)\,dt \qquad (2)$$

where λ is the wavelength of the spatially coherent illumination, f is the focal length of both lenses L_1 and L_2, and the spatial frequency ν is related to the horizontal displacement, x_2, on plane P_2 by[9]

$$\nu = x_2/\lambda f \qquad (3)$$

By an appropriate choice of an input, this coherent processor will be shown to have the capability of ambiguity function display.

Consider, then, the one dimensional temporal signal $f(t)$ in Fig. 2a and its representation on the (t,τ) plane [Fig.2b]. By rotating this function counterclockwise about the origin an angle of θ [Fig.2c], we generate the function

$$f[t\cos\theta + \tau\sin\theta]$$

Thus, for a rotation of 45 degrees, we obtain $f\{(t+\tau)/\sqrt{2}\}$, and for a rotation of -45 degrees, we obtain $f\{(t-\tau)/\sqrt{2}\}$. If we cascade transparencies of these two functions, in the input plane of the processor of Fig.1 so as to form the product $f[t+\tau)/\sqrt{2}]\ f[t-\tau)/\sqrt{2}]$, then, from Eq.2, the resulting output is

$$\begin{aligned} U(\nu,\tau) &= \exp(-j2\pi\lambda f\nu^2) \\ &\quad \cdot \int_{-\infty}^{\infty} f\left[\frac{t-\tau}{\sqrt{2}}\right] f\left[\frac{t+\tau}{\sqrt{2}}\right]\exp(-j2\pi\nu t)\,dt \\ &= \sqrt{2}\exp[-j2\pi\nu(\tau+\lambda f\nu)] \\ &\quad \int_{-\infty}^{\infty} f(t')f(t'-\sqrt{2}\tau)\exp[-j2\pi(\sqrt{2}\nu)t']\,dt' \end{aligned} \qquad (4)$$

where we have made the change of variable

$$t' = \frac{t+\tau}{\sqrt{2}}$$

The intensity distribution associated with Eq.4 is immediately recognized as a scaled version of the squared modulus of the ambiguity function:[10]

$$\begin{aligned} I(\nu,\tau) &= |U(\nu,\tau)|^2 \\ &= 2|\chi(\sqrt{2}\nu,\sqrt{2}\tau)|^2 \end{aligned} \qquad (5)$$

Experimental Results

To evaluate the performance of the proposed processor, the ambiguity functions for a single and double pulse signal are evaluated analytically and compared to the corresponding optical system outputs. In practice, the processor output is magnified by conventional means for observation and photographic purposes.

For a Single Pulse

For a single pulse, (Fig.3a), we may write

$$f(t) = \text{rect}\,(t/2T) \qquad (6)$$

where 2T is the pulse duration and

$$\text{rect}\,(t) \triangleq \begin{cases} 1 \; ; & |t| \leq 1/2 \\ 0 \; ; & t > 1/2 \end{cases}$$

The geometric interpretation of f(t), $f\{\frac{t+\tau}{\sqrt{2}}\}$, and $f\{\frac{(t+\tau)}{\sqrt{2}}\} f\{\frac{(t-\tau)}{\sqrt{2}}\}$ are shown in Figs.3b, 3c and 3d respectively.

Substituting Eq.6 into Eq.1 followed by evaluation yields the ambiguity function

$$\chi(\nu,\tau) = \begin{cases} (2T - |\tau|)\,\text{sinc}\,\nu(2T - |\tau|)\exp(-j\pi\nu\tau); & |\tau| \leq 2T \\ 0 & ; |\tau| \geq 2T \end{cases} \tag{7}$$

where $\text{sinc}\,\nu \triangleq (\sin \pi\nu)/\pi\nu$. The corresponding output intensity is

$$|\chi(\nu,\tau)|^2 = \begin{cases} (2T - |\tau|)^2 \text{sinc}^2\nu(2T - |\tau|) \; ; & |\tau| \leq 2T \\ 0 \; ; & |\tau| \geq 2T \end{cases} \tag{8}$$

For purpose of identification, it is instructive to examine the locus of points where the ambiguity function is identically zero. From Eq.8, this zero value locus may easily be shown to be

$$\nu = \frac{n}{2T - |\tau|} \quad ; \quad |\tau| \leq 2T \tag{9}$$

where n is any non-zero integer. The piecewise hyperbolic nature of these curves is shown in Fig.4.

The ambiguity function for a single pulse is generated by appropriately rotating two identical thin slits in plane P_1 of the coherent optical processor of Fig.2. The result is shown in Fig.5. As can be seen, the coherent processor output compares quite nicely with the theoretical result in Fig.4. A three-dimensional computer graph of the corresponding ambiguity function modulus may be found in Fig. 6.6 of Rihaczek.[11]

For a Double Pulse

For a double pulse, (Fig.6a), we write

$$f(t) = \text{rect}\{(t + 2T)/2T\} + \text{rect}\{(t-2T)/2T\} \tag{10}$$

where, for convenience, the pulse separation, 2T, has been chosen to be equal to each of the pulse widths. The geometrical interpretation of $f\{\frac{(t-\tau)}{\sqrt{2}}\} f\{\frac{(t+\tau)}{\sqrt{2}}\}$ is shown in Fig.6b. The ambiguity function associated with the double pulse is

$$\chi(\nu,\tau) = \begin{cases} 2(2T - |\tau|)\text{sinc}\,\nu(2T - |\tau|) \\ \qquad \cos(4\pi T\nu)\exp(-j\pi\tau\nu) \; ; & |\tau| \leq 2T \\ -(2T - |\tau|)\text{sinc}\,\nu(2T - |\tau|)\exp(-j\pi\tau\nu) \\ \qquad ; & 2T \leq |\tau| \leq 4T \\ (6T - |\tau|)\text{sinc}\,\nu(6T - |\tau|)\exp(-j\pi\tau\nu) \\ \qquad ; & 4T \leq |\tau| \leq 6T \\ 0 \; ; & |\tau| \geq 6T \end{cases} \tag{11}$$

The corresponding output intensity is

$$|\chi(\nu,\tau)|^2 = \begin{cases} 4(2T - |\tau|)^2\text{sinc}^2\nu(2T - |\tau|) \\ \qquad \cos^2(4\pi T\nu) \; ; & |\tau| \leq 2T \\ (2T - |\tau|)^2\text{sinc}^2\nu(2T - |\tau|) \\ \qquad ; & 2T \leq |\tau| \leq 4T \\ (6T - |\tau|)^2\text{sinc}^2\nu(6T - |\tau|) \\ \qquad ; & 4T \leq |\tau| \leq 6T \\ 0 \; ; & |\tau| \geq 6T \end{cases} \tag{12}$$

The equations describing the zero-value loci are easily shown to be

$$\begin{aligned} \nu &= (2m + 1)/8T \quad ; \quad |\tau| \leq 2T \\ \nu &= n/(|\tau| - 2T) \; ; \quad |\tau| \leq 4T \\ \nu &= n/(6T - |\tau|) \; ; \quad 4T \leq |\tau| \leq 6T \end{aligned} \tag{13}$$

where m is any integer and, as before, n is any non-zero integer. An illustration of these zero-value loci is presented in Fig.7.

By appropriately placing two identical double slits in planes P_1 and P_2 of the coherent processor, the ambiguity function for the double pulse is generated. The result, shown in Fig.8, again compares quite favorably with the theory.

An Alternate Scheme

The coherent processor just discussed, is capable of displaying the ambiguity function only in magnitude. That is, quadratic and linear phase factors are present on the output plane [see Eq.4].

A processor capable of generating the ambiguity function both in magnitude and phase is presented in Fig.9. In plane P_1, we place the transparency $f\{\frac{(\tau - t)}{\sqrt{2}}\}$ which is formed by the previously discussed 45 degree rotation of f(t), followed by coordinate reversal (rotating $f\{\frac{(t-\tau)}{\sqrt{2}}\}$ 180 degrees about the t and τ axes). The scaling lenses L_1 and L_2 have respective focal lengths related by

$$f_1 = \sqrt{2}\, f_2 \tag{14}$$

The field amplitude incident on the left of plane P_2 is the desired $f(t - \tau)$. This will multiply the transmittance f(t) in plane P_2 to give immediately to the right of P_2 the field amplitude $f(t)f(t - \tau)$. The geometrical interpretation of this product in the (t,τ) plane, for the case of a single pulse, is shown in Fig.10.

With reference to Eq.1, it remains to perform a Fourier transformation with respect to t. This is accomplished with cylindrical lenses L_a, L_b, and L_c which have respective focal lengths of

$$2f_a = f_b = 2f_c \tag{15}$$

One sees that, from plane P_2 to P_3, imaging is performed in the vertical direction by L_a and L_c while Fourier

transformation is independently performed in the horizontal direction by L_b. Thus, the field amplitude, $U(\nu,\tau)$, in plane P_3 is a scaled version of the ambiguity function:

$$U(\nu,\tau) = \int_{-\infty}^{\infty} f(t)f(t-\tau)\exp(-j2\pi\nu t)\,dt \qquad (16)$$

$$= \chi(\nu,\tau)$$

where ν is related to the horizontal displacement, x_3, in P_3 by

$$\nu = x_3/\lambda f \qquad (17)$$

This ambiguity function processor, which is more elaborate than that shown in Fig.2, need be used only when the ambiguity function's magnitude and phase are required.

As a final note, we observe that the scheme we propose assumes that $f(t)$ is real valued. If, in fact, $f(t)$ is complex, then we need to generate $f^*(t-\tau)$ in the integrand of Eq.1 in order to properly generate $\chi(\nu,\tau)$. Some additional work appears needed for the case of a general complex-valued $f(t)$.

Acknowledgements

This research was supported by the Air Force Office of Scientific Research, Air Force Systems Command, USAF, under grant AFOSR-75-2855A.

References

1. P.M. Woodward, Probability and Information Theory, With Applications to Radar (Pergamon Press, Oxford, 1963).
2. A. Papoulis, J. Opt. Soc. Am. 64 779 (1974).
3. L.J. Cutrona, E.N. Leith, C.J. Palermo, and L.J. Porcello, IRE Trans. on Info. Theory, IT-6 386 (1960).
4. L.J. Cutrona in Optical and Electro-Optical Information Processing, J.T. Tippet et.al., eds. (MIT Press, 1965).
5. K.Preston, Coherent Optical Computers (McGraw-Hill, New York, 1972).
6. The "ambiguity function processors" in Refs. (4-5, 1-3) should rigorously be called uncertainty function processors in that they are only capable of displaying the uncertainty function $|\chi(\nu,\tau)|$. Following this precedent, we herein refer to both $\chi(\nu,\tau)$ and $|\chi(\nu,\tau)|$ as the ambiguity function. The actual function to which reference is made is clear in the context of the paper.
7. D. Casasent and F. Casasayas, Appl. Opt. 14 1364 (1975).
8. M.C. Bartlett, L.W. Couch, and R.C. Johnson, Proc. IEEE 63 1625 (1975).
9. J.W. Goodman, Introduction to Fourier Optics (McGraw-Hill, New York, 1968).
10. The squared modulus of the ambiguity function is sometimes also referred to as the ambiguity function.
11. A.W. Rihaczek, Principles of High Resolution Radar (McGraw-Hill, New York, 1969).

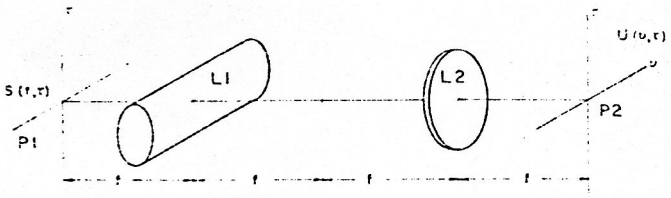

Fig.1. A coherent processor for ambiguity function display. Both the lenses have focal length f. Fourier transformation is performed in the horizontal direction and imaging in the vertical direction.

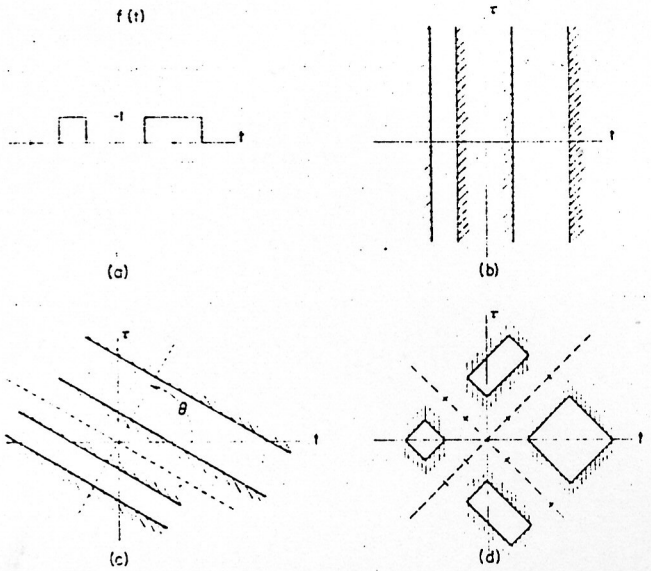

Fig.2. (a) A function $f(t)$ in time and (b) on the (t,τ) plane. (c) By rotating $f(t)$ counterclockwise an angle of θ about the origin of the (t,τ) plane, we generate $f(t\cos\theta + \tau\sin\theta)$. (d) The function $f\{\frac{(t+\tau)}{\sqrt{2}}\}f\{\frac{(t-\tau)}{\sqrt{2}}\}$ in the (t,τ) plane.

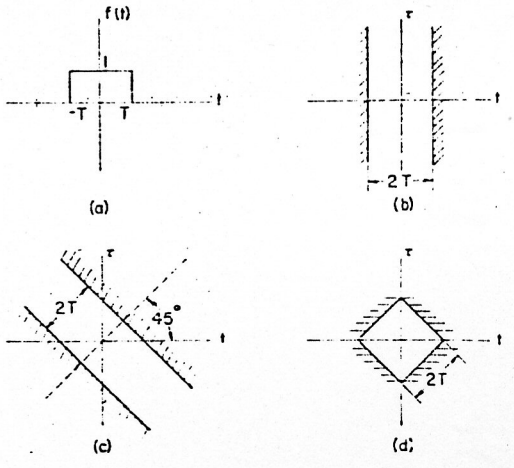

Fig.3. A single pulse, (a) in time, (b) on the (t,τ) plane, (c) rotated 45 degrees on the (t,τ) plane to form $f\{\frac{(t+\tau)}{\sqrt{2}}\}$, (d) the product of two pulses rotated 45 degrees and -45 degrees on the (t,τ) plane to form $f\{\frac{(t+\tau)}{\sqrt{2}}\}f\{\frac{(t-\tau)}{\sqrt{2}}\}$.

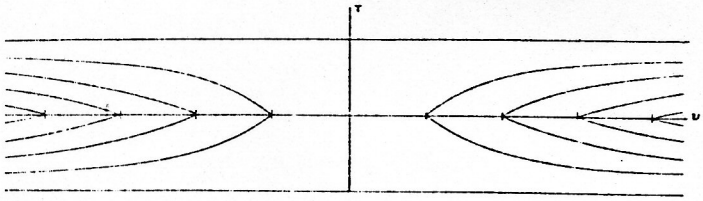

Fig.4. Zero locus plot of the ambiguity function of a single pulse.

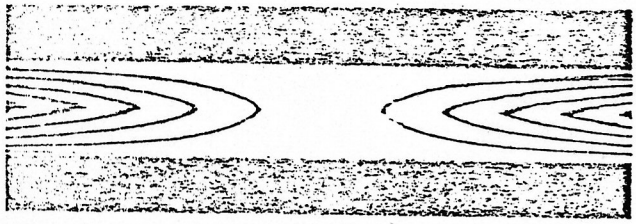

Fig.5. The ambiguity function (modulus squared) display for a single pulse, as generated by the coherent processor of Fig.2.

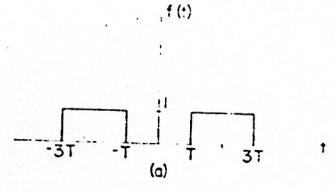

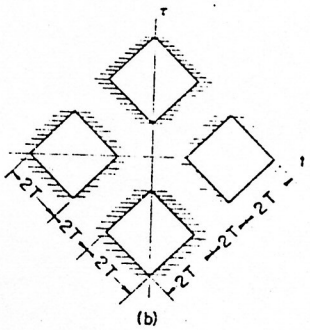

Fig.6. (a) A double pulse. (b) The corresponding function $f\{\frac{(t+\tau)}{\sqrt{2}\tau}\}f\{\frac{(t-\tau)}{\sqrt{2}\tau}\}$ on the (t,τ) plane.

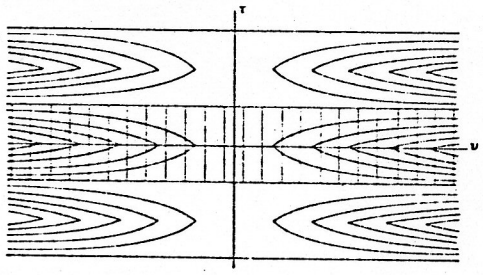

Fig.7. Zero locus plot of the ambiguity function of a double pulse.

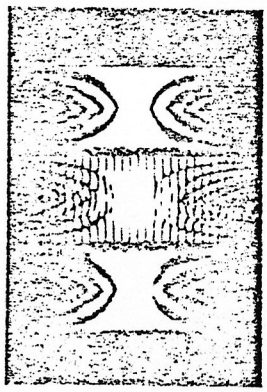

Fig.8. The ambiguity function (modulus squared) display for a double pulse as generated by the coherent processor of Fig.2.

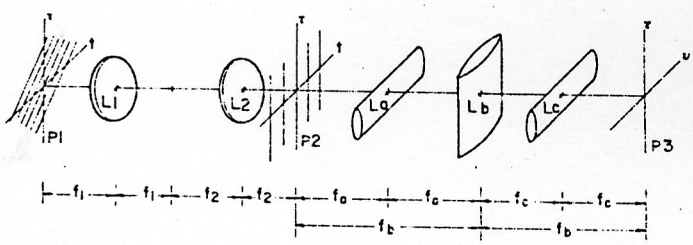

Fig.9. Coherent processor for generating the ambiguity function in phase and amplitude. Scaling lenses L_1 and L_2 have a focal length relation $f_1 = \sqrt{2}f_2$.

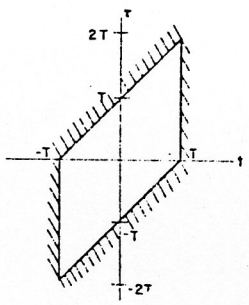

Fig.10. The product $f(t)f(t-\tau)$ on the (t,τ) plane for the single pulse of Fig.3a.